Estimation of reservoir porosity based on seismic inversion results using deep learning methods

Feng, Runhai

DOI
10.1016/j.jngse.2020.103270

Publication date
2020

Document Version
Final published version

Published in
Journal of Natural Gas Science and Engineering

Citation (APA)
Feng, R. (2020). Estimation of reservoir porosity based on seismic inversion results using deep learning methods. *Journal of Natural Gas Science and Engineering*, *77*, Article 103270. https://doi.org/10.1016/j.jngse.2020.103270

Journal of Natural Gas Science and Engineering 77 (2020) 103270

Contents lists available at ScienceDirect

Journal of Natural Gas Science and Engineering

journal homepage: http://www.elsevier.com/locate/jngse

Estimation of reservoir porosity based on seismic inversion results using deep learning methods

Runhai Feng

Department of Geoscience and Engineering, Delft University of Technology, Delft, 2628CN, the Netherlands

ARTICLE INFO

Keywords:
Seismic inversion
Deep learning
Reservoir porosity
Vienna basin

ABSTRACT

Location limitation of logged wells restricts the porosity estimation across the whole reservoir target, whereas seismic data are always collected to cover larger areas. In this paper, inversion results of seismic data are proposed as inputs for the prediction of reservoir porosity, even though the resolution is decreased, compared with well-log readings. The non-linear inversion scheme used is able to explore the complex relationship between rock properties and seismic data, which could potentially provide a higher quality of inversion results. As a regression process, Convolutional Neural Networks is then applied to estimate the reservoir porosity, based on the outputs of seismic inversion scheme. Incorporating 2D kernel filters which are convolved with input rock properties, the local information inside filters window is considered, and a better prediction performance is to be guaranteed. This is due to the fact that reservoir porosity is formed under depositional and digenetic rules, and it is intrinsically correlated with rock properties along the vertical direction in a short range. The designed workflow is applied to a real dataset from the Vienna Basin where compressibility and shear compliance are inverted and then used as inputs for the porosity estimation by Convolutional Neural Networks. For a comparison, the traditional Artificial Neural Networks is also trained and applied to the same dataset. It is concluded that the Convolutional Neural Networks can achieve a higher accuracy, and a 3D cube of reservoir porosity is obtained without location restriction of well logs.

1. Introduction

Reservoir characterization is an essential step in the development of hydrocarbon reservoirs, and different reservoir parameters are to be determined during this process, such as porosity, permeability and fluid saturation, which are involved in almost all calculations related to the reservoir production (Na'imi et al., 2014). Laboratory measurements of cored wells or logging data could provide high-resolution values of these parameters. However, only isolated locations could be assessed because of the limited budget and consumed time. On the other hand, 2D or 3D information is available in seismic data over an area typically covering the extent of the target reservoir. Through an inversion of seismic data, rock properties and subsurface structures are able to be inferred and imaged. Here, an effort is presented to estimate one of the reservoir parameters — porosity, which is a quantification factor for the storage of hydrocarbon reservoirs (Yu et al., 2018), from a reservoir-oriented elastic wave-equation based inversion of seismic data.

In order to explore the relationship between reservoir porosity and rock properties (compressibility and shear compliance), different methodologies could be employed, of which deep learning has attracted particular interests among geoscientists, for its ability to automate interpretation and inversion of well-log data. As a subclass of machine learning, the algorithms of deep learning use a number ('depth') of hidden layers to progressively extract high-level features from raw inputs (Deng and Yu, 2014). Convolutional Neural Networks (CNN), a special form of deep learning methods, includes a convolution operator as part of its framework (Das et al., 2019), and is capable to bring the field of image classification and computer vision to a new level (Lima et al., 2019). Wu and McMechan (2018) modified full-waveform inversion by incorporating a CNN in order to capture the geometrical targets. Wu et al. (2018) proposed a fast prediction of permeability from images, which is enabled by image recognition neural networks. Based on a supervised CNN, Yang and Ma (2019) built velocity models directly from raw seismograms.

Rather than for typical classification problems, CNN is to be used here for the porosity estimation in a regression process. In addition, to make a comparison, Artificial Neural Networks (ANN) is also applied, which is inspired by the biological system consisting of structures of

E-mail addresses: r.feng@tudelft.nl, mychen007@126.com.

https://doi.org/10.1016/j.jngse.2020.103270
Received 28 November 2019; Received in revised form 18 February 2020; Accepted 17 March 2020

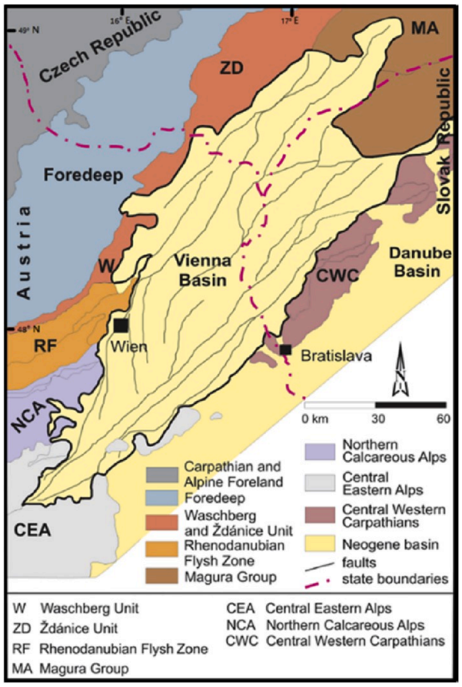

Fig. 1. Simplified geological map of the Vienna Basin (modified after Kováč et al., 2008).

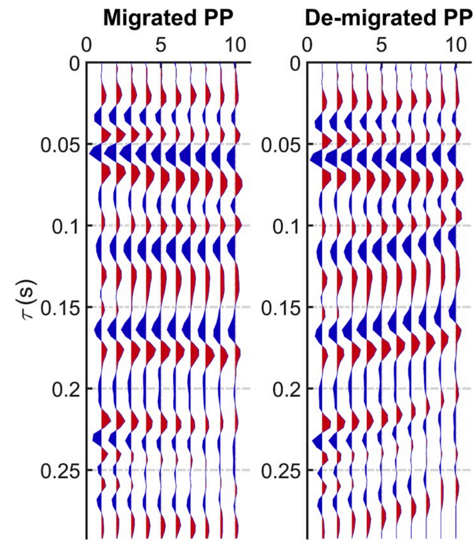

Fig. 3. Migrated and de-migrated seismic gathers, of which the later one will be the input for the non-linear inversion scheme. Red color in wiggle traces means a positive amplitude associated with increased rock impedances (peak); blue color is related with a negative amplitude of decreased rock impedances (trough).

interconnected neurons (Bishop, 1995), and has been widely used in geophysical problems as well. For example, with the help of ANN, synthetic well logs have been generated by Rolon et al. (2009) to analyze the reservoir properties in areas where the set of logs is absent or incomplete. Jozanikohan et al. (2015) predicted the clay volume by multilayer perceptron neural network (a special case of ANN), for its important impact on the production potential in shaly sand reservoirs.

Instead of using seismic attributes or AVO (amplitude vs. offset) inverted impedance as inputs, it is suggested in this paper to determine reservoir porosity based on the results from full-waveform inversion (FWI), which could provide a higher resolution of rock properties in the subsurface. FWI tries to incorporate different types of waves such as refractions and multiples into the optimization process, in order to extract quantitative information from seismograms based on a full-wavefield modelling (Tarantola, 1984; Virieux and Operto, 2009). Treister and Haber (2017) used a joint FWI and travel-time inversion to obtain a smooth model for a good approximation for the true model. With an increasing availability of longer-offset seismic data, successful examples of FWI include Yang et al. (2016) who applied ocean-bottom-cable data to quantify changes in reservoir properties at the Valhall field of North Sea.

Different with the FWI scheme mentioned above, the technique of non-linear inversion method presented here is based on an integral representation of the full-elastic wave equations. All internal transmission effects and internal multiple scatterings/mode conversions are considered. The order of multiples used in the inversion process is determined by the number of iterations. Since the non-linear relationship between rock properties and seismic data is exploited, this inversion scheme could guarantee a good recovery of the subsurface properties, as well as the layer geometries (Gisolf and van den Berg, 2010a, 2010b). Therefore, results from the non-linear inversion scheme are better candidate inputs for the prediction of reservoir porosity.

The context of this paper will be organized as follows: Firstly, a short overview of the geological settings and dataset of the Vienna Basin is being presented; then the mentioned inversion scheme is described briefly and applied to the pre-processed seismic data; subsequently with the incorporation of well logging data, the relationship between inversion results and reservoir porosity is investigated by CNN and ANN, for a comparison. Finally, discussions and conclusions are made.

The main objective in this paper is to propose a workflow that is from seismic inversion results to reservoir parameters, in order to circumvent the location limitation of well logs. Meanwhile, possibilities for application of state-of-the-art deep leaning methods to the dataset at hand

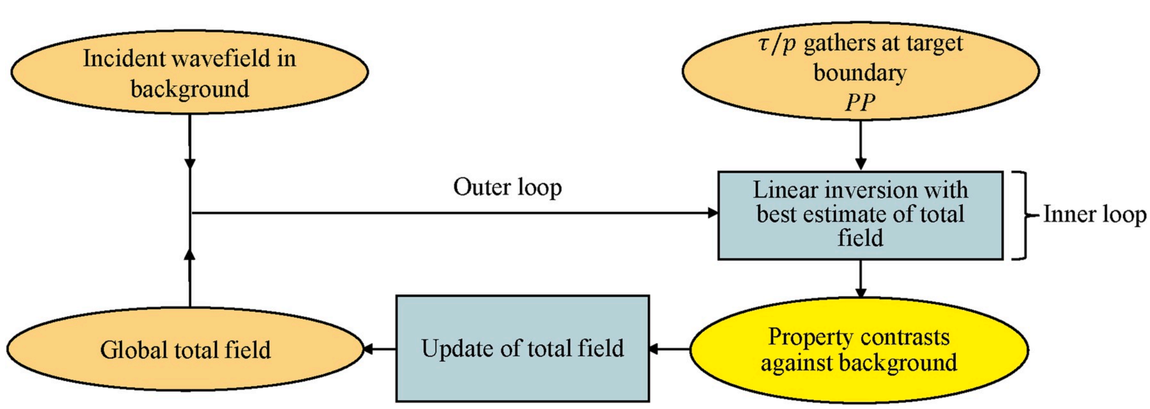

Fig. 2. Schematic flow chart of the non-linear inversion scheme (Gisolf et al., 2014; Feng et al., 2017).

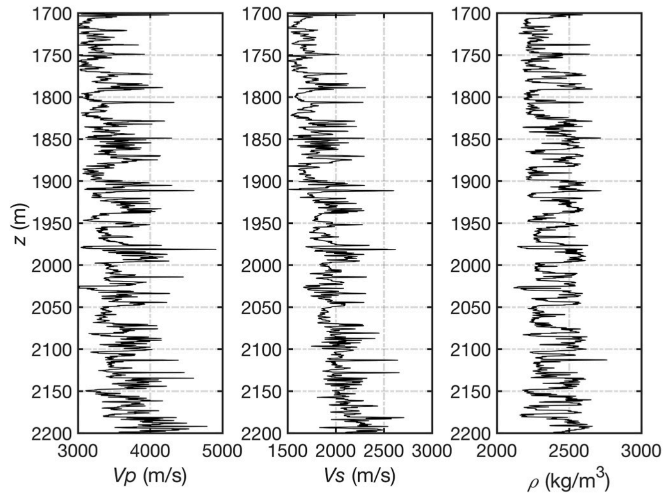

Fig. 4. Rock property data at Well_01, in terms of P- and S-wave velocities (V_P, V_S), and density (ρ).

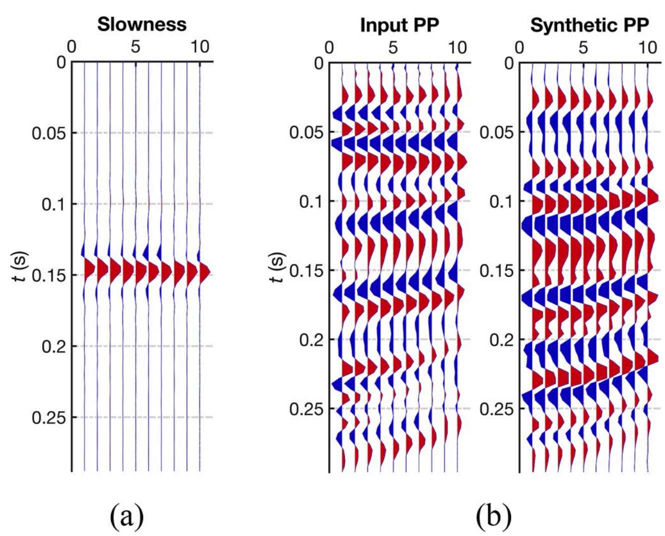

Fig. 5. (a) Extracted wavelet with ten slownesses; (b) Input and synthetic PP seismic gathers, of which input gathers for the seismic inversion are the outputs of de-migration, and the synthetic gathers are obtained based on the well logs (Well_01, Fig. 4) and extracted wavelet (Fig. 5a) using the Kennett invariant embedding method (Kennett, 1983; Feng et al., 2015a).

will be investigated.

2. Geological setting and dataset

In order to demonstrate the proposed workflow, a dataset from the Vienna Basin in Austria is selected, in which clastic reservoirs are explored. As an extensional basin, the Vienna Basin is between the Eastern Alps and Western Carpathians (Fig. 1) (Strauss et al., 2006). The basin fill consists of shallow marine and terrestrial sediments of Early to Middle Miocene age up to 5500 m thick in the central parts (Strauss et al., 2006). Main reservoirs in this basin are from the Sarmatian (SH) and Badenian (TH) time during which the transport directions of sediments were from the Northwest along the Zaya Channel, and also from the Northeast along the ancient "Ur-March" river (Kováč et al., 2008).

A single dataset VBSM (Vienna Basin Super Merge) has been built based on vintages of 3D seismic surveys acquired in different years. The potential reservoir units in this area are oil and gas sands, in which the porosity is generally above 20%. Wells have been drilled reaching the hydrocarbon zone around 2 km in depth, with different loggings such as density, compressional and shear velocities etc. They are the basis for a standard petrophysical evaluation and calibration. However, only sparse locations could be accessed, and therefore, inversions from seismic data are used here for the porosity prediction, in which neural networks will be employed to fully honor the complex relationship within the data, instead of typical rock physical models being assumed (Avseth et al., 2010).

3. Inversion scheme and data pre-processing

The inversion scheme applied here was developed by Gisolf & van den Berg (2010a, 2010b), and the acoustic mode was implemented by Tetyukhina et al. (2014) on a synthetic geological and petrophysical model of Book Cliffs, USA. After the wave-mode conversions have been taken into account, the new inversion scheme is based on the full-elastic wave equations and has been applied by Feng et al. (2015b, 2017) on a more detailed model of Book Cliffs. Since all internal multiples and wave-mode conversions have been included in the inversion process, it allows a recovery of broadband properties and a high resolution of inversion results is provided (Gisolf et al., 2014; Feng et al., 2016a, 2016b). A short summary of the inversion scheme as well as data pre-processing is given below.

3.1. Non-linear inversion scheme

Based on an integral representation of the full-elastic wave equations, the so-called scattering integral (Fokkema and van den Berg, 1993), the non-linear relationship is being exploited between acquired seismic data and elastic properties to be estimated. An iterative procedure is used to solve this problem. The total wavefield in the object from our best knowledge of the properties and the updated properties from the data is determined alternatively (Gisolf et al., 2014; Feng et al., 2017). Rather than in a constant background medium, the total wavefield is obtained in the full inhomogeneous medium. Its first estimate is the incident field that propagates in the background models, which is a well-known linearization of the problem called the Born approximation (Fokkema and van den Berg, 1993). The backgrounds are smooth media in which the incident field and Green's functions are calculated (Haffinger, 2013). They are the prior knowledge before the inversion, which can be obtained from migration velocities, well logs or even empirical rock physical considerations (Feng et al., 2017).

Properties in the object are estimated linearly with the first estimated total wavefield and seismic data in the inner loop. Then the total wavefield will be updated in the outer loop based on wave equations, which will contain the first-order scattering. The linear inversion of properties and forward modelling to incorporate an increased order of scattering are alternated subsequently (Fig. 2). The order of multiples accounted for in the data is determined by the number of iterations, which will stop when neither the properties nor the total wavefield change significantly (Gisolf and Verschuur, 2010; Tetyukhina et al., 2014).

In the non-linear inversion scheme, outputs are the contrasts in terms of compressibility ($\kappa = 1/K$, with K being the bulk modulus), shear compliance ($M = 1/\mu$, with μ being the shear modulus) and density (ρ) based on the backgrounds (κ_0, M_0, ρ_0):

$$\chi_\kappa = \frac{\kappa - \kappa_0}{\kappa_0} \tag{1}$$

$$\chi_M = \frac{M - M_0}{M_0} \tag{2}$$

$$\chi_\rho = \frac{\rho - \rho_0}{\rho_0} \tag{3}$$

The P and S velocities can be expressed in elastic moduli (κ and M):

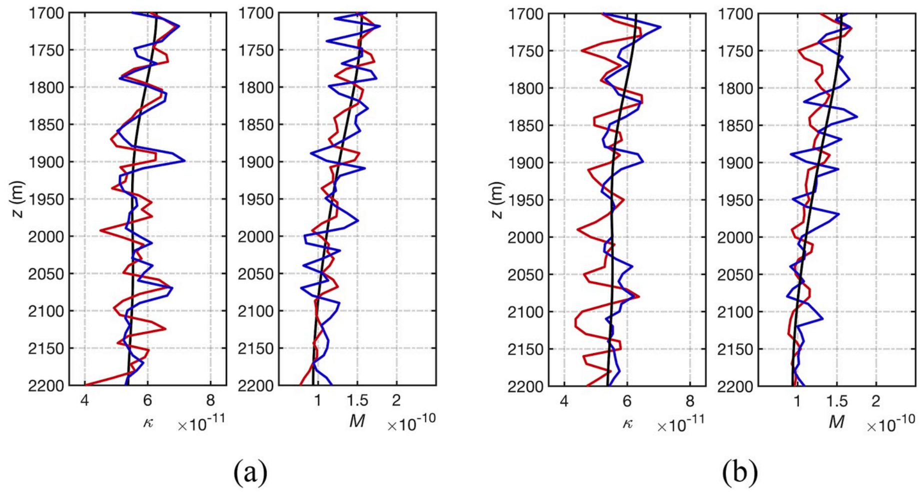

Fig. 6. (a) True (red curve) and inverted (blue curve) rock properties at Well_01. (b) A blind test at Well_02 with true (red curve) and inverted (blue curve) rock properties. The black curve represents the smooth background media.

$$V_P = \sqrt{\frac{1}{\rho}\left(\frac{1}{\kappa} + \frac{4}{3M}\right)} \tag{4}$$

$$V_S = \sqrt{\frac{1}{M\rho}} \tag{5}$$

The elastic moduli (κ and M) are in the wave equations intrinsically and are deemed to relate more directly to rock types when reservoir lithologies are the desired targets (Feng et al., 2018a, 2018b).

3.2. Data pre-processing

The proposed inversion scheme is reservoir-oriented, and effects of the overburden have to be removed. In the studies presented by Tetyukhina et al. (2014) and Feng et al. (2017), virtual seismic receivers have been placed on top of the reservoir target interval. Therefore, the overburden effects have been assumed to be compensated for. In this real case study, extensive pre-processing needs to be performed in order to select the desired seismic data subset.

Inputs to the pre-processing are the pre-stack migrated seismic gathers and an interpreted horizon. As a stratigraphical layer's boundary, horizon is the top of the interested reservoir interval and can be identified on a migrated image. A smaller seismic cube is then extracted based on the marked horizon and desired time window. In order to remove dipping noises in the selected seismic sub-cube, a dip filter is applied, since large structural dips in the reservoir target are not expected (Haffinger et al., 2015). The filtered seismic data are then transformed from the offset to the Radon domain (τ/p), and de-migrated over the reservoir interval, according to the following steps: (1) calculate the shifting time for seismic events with a help of the smooth velocity model; (2) interpolate the gathers per slowness ($p = \sin(\theta)/Vp$, in which θ is the incidence angle, Vp is the average P-wave velocity across the whole section). This is possible when dealing with a plane wave (τ/p) domain, assuming a layered medium immediately below the target surface (Haffinger et al., 2015). It is also the same assumption made in the inversion scheme which is 1D or 1.5D, if the 2D wavefield (de-migrated PP in Fig. 3) is considered (Gisolf et al., 2014). Working in a trace-by-trace mode ensures that the geological 3D dip is honored by the data (Feng et al., 2017). Overburden transmission effects could be accounted for through seismic-to-well matches (Gisolf et al., 2014).

In the migrated PP (pressure-to-pressure) reflected seismic data (Fig. 3), all seismic events should be horizontal (gather flattening) after migration, which would allow a subsequent amplitude vs. offset or angle (AVO or AVA) analysis. While the de-migration would map these events to their "original recording times" across the slowness domain, which are tilted up. The de-migrated data will be compared with the full-waveform simulated results from the non-linear inversion scheme to update model parameters accordingly.

4. Seismic inversion results

Before an implementation of the proposed inversion scheme, the algorithm needs to know the source wavelet in order to calculate the incident wavefield in the first iteration. A broadband synthetic seismic data based on the well data (Well_01) (Fig. 4) have been generated using the Kennett method (Kennett, 1983), which is an exact solution of wave equations and able to take care of all the internal multiples, as well as the wave-mode conversions and transmission effects (Haffinger, 2013; Feng et al., 2017). The wavelet extraction is performed by a least-square matching between the broadband synthetics and real data at the well location (Fig. 5a) (White, 2003; Haffinger, 2013).

However, the seismic-to-well match is rather poor especially in the lower part, while it is quite good in the upper part (Fig. 5b), which might be caused by the fact that the location of real seismic data does not ideally coincide with the selected well location (Well_01). And also, there are deviations in the trajectory path of the well. It is the similar case in other geophysical explorations, since there is always some distance between seismic survey lines and deviated wells over the field.

After applying the proposed inversion scheme, the inversion results at Well_01 are shown in Fig. 6a. The inverted properties have been transformed into their absolute values (Eqn. (1), (2) and (3)). The smooth background media have been obtained with a high-cut filter on the true logs and have been kept constant for all locations. When more wells are available, a simple interpolation could create this low-wavenumber background model.

As expected, the inversion quality is suboptimal since the seismic-to-well match is poor, even though the inverted κ matches the truth quite well in the upper part. It can also be realized that the inversion quality of κ is better than that of M generally, since only PP data are available here. In the synthetic case study presented by Feng et al. (2017), the inversion qualities of κ and M are almost equally good, since PP (pressure-to-pressure) and PS (pressure-to-shear) data are used together. Density is skipped here due to the poor data quality (Fig. 5b), which means that all three elastic parameters (κ, M, ρ) cannot be estimated reliably (Haffinger, 2013).

In the next step, the inversion at another well location (Well_02) is performed as a blind test (Fig. 6b). The results are mediocre because of the mentioned problem in the seismic-to-well match (Fig. 5b). Their

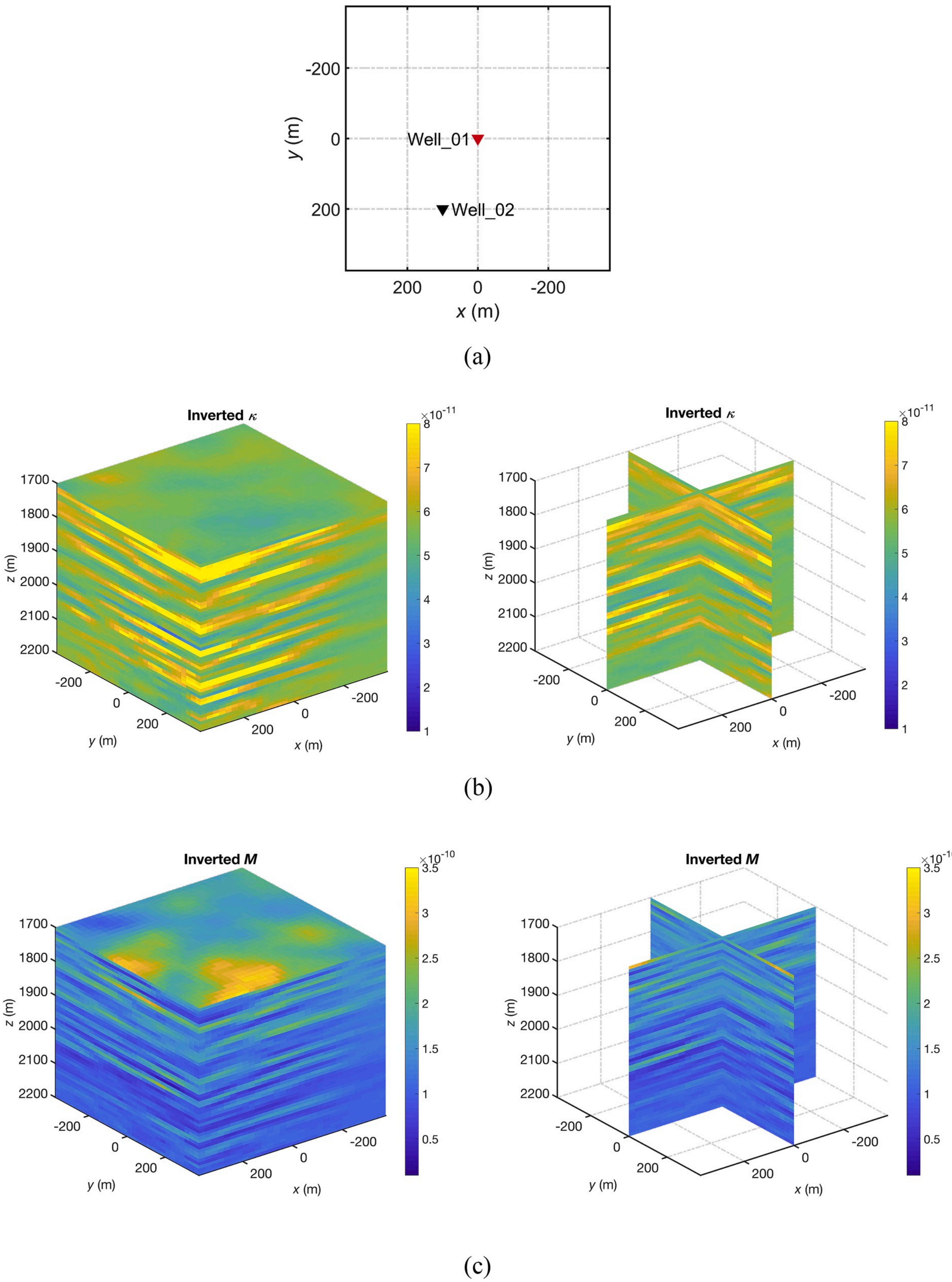

Fig. 7. (a) Schematic view of the two well locations (Well_01, Well_02). Inverted κ (b) and M (c) in 3D cubes and two slices.

original well logs have been upscaled to the seismic resolution, in order to obtain the truth in Fig. 6.

With 3D seismic data used, inversion results in cubes are shown in Fig. 7b and c, together with two slices along the inline and crossline directions, for an inspect of internal structures. The top boundary of the property cubes is the marked horizon, and a time-to-depth conversion is made. The relative location of Well_01 and Well_02 is shown in Fig. 7a.

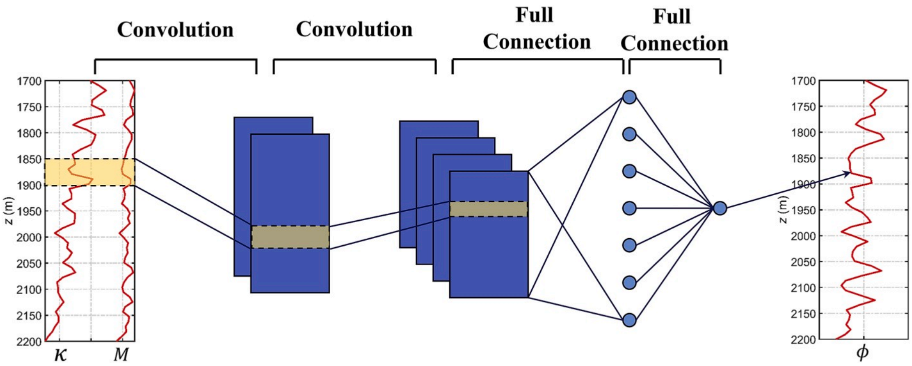

Fig. 8. Structure of 2D CNN for the porosity prediction based on two input features of κ and M.

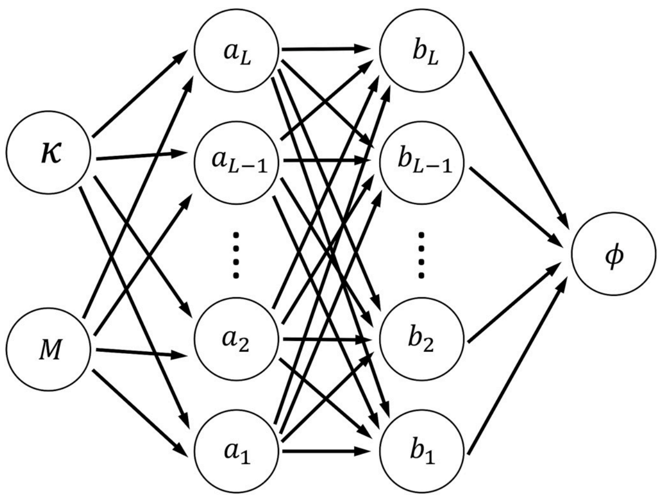

Fig. 9. Architecture of ANN for the prediction of porosity.

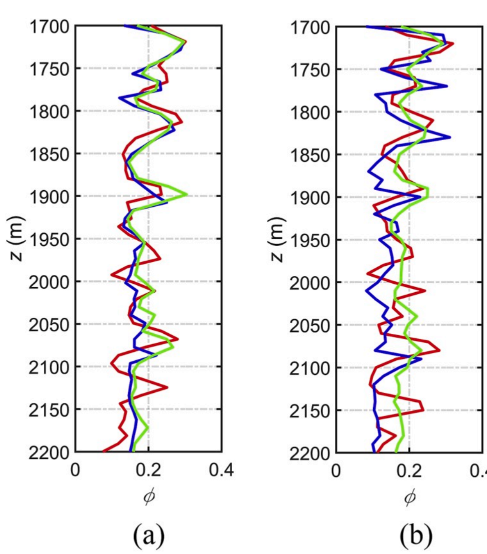

Fig. 10. Predicted porosity at Well_01 (a) and Well_02 (b). Blue curves show results by ANN and green curves represent results by CNN. The truth is in red, which is derived after upscaling of the original logs to the seismic resolution. Correlation coefficient is 0.5847 for ANN, 0.6624 for CNN at Well_01 (a); 0.3248 for ANN, 0.5574 for CNN at Well_02 (b).

5. Porosity prediction

Featured by convolutional layers, Convolutional Neural Networks (CNN) has gained increasing popularity to solve problems including image classification and object detection (Biswas et al., 2019). With different activation functions applied, classification or regression can be performed by CNN individually, which might outperform other conventional networks, such as Artificial Neural Networks (ANN) (Bishop, 1995), since local information has been considered. In this paper, a 2D CNN is designed for the estimation of continuous porosity in a regression process (Fig. 8). The layer input is the inverted κ and M from seismic data (Fig. 7b and c). The architecture of designed CNN includes two convolutional layers with 12 and 24 filters respectively. The width of kernel filters is selected as comparable to the wavelength corresponding to the central frequency of the extracted wavelet, which is a natural fit to the seismic inversion problem, as the recorded seismic data are usually modelled as a wavelet convolved with the reflectivity series (Das et al., 2019). Stride of the convolutional filters shifting over the input volume is set as 1 and no padding (valid) is used. Two full connections are then made, in which there are 48 neurons in the first connected layer, and one neuron is allocated in the second layer, which is related to the target porosity.

Besides, ANN, the brain-inspired system (Bishop, 1995), is also applied, for a comparison with CNN (Fig. 9). Two hidden layers have been allotted with 100 neurons each, and the collection of connected units is able to loosely model biological neurons. Signal is transmitted through the connections ("edges") to other synaptic neurons, and the associated neural parameters are adjusted as learning proceeds.

In the above designed networks (CNN and ANN), the nonlinear rectified linear unit (ReLU) function is adopted for the implementation of layers activation and to introduce the nonlinearity, as defined by $f(x) = \max(0, x)$ (Nair and Hinton, 2010). Operating on the output layer, the *sigmoid* function (Gibbs and MacKay, 2000) will map all the values into the porosity range between 0 and 1. The mean-squared error is selected as the loss function to measure the difference between prediction from the network and truth from the labeled porosity. A dropout ratio of 25% has been assigned in order to regularize these networks and prevent overfitting. Initial weights in these hidden layers are randomly assigned using the Xavier initialization (Glorot and Bengio, 2010), and initial biases are set to 0 before training of the systems. To update neural weights and biases, Adam algorithm is used (Kingma and Ba, 2014).

True data at the two wells (Well_01 and Well_02) have been randomly split into training (80%), validation (10%) and test (10%) subsets, to determine and tune neural parameters, as well as to examine the generalization capability of trained systems. In total, there are 6834 data samples, which are believed to be representative enough for the porosity distribution in the selected reservoir target, and the complex relationship between rock properties and reservoir porosity is expected be well explained by the neural systems. Furthermore, data synthetization and augmentation would also be helpful for the training

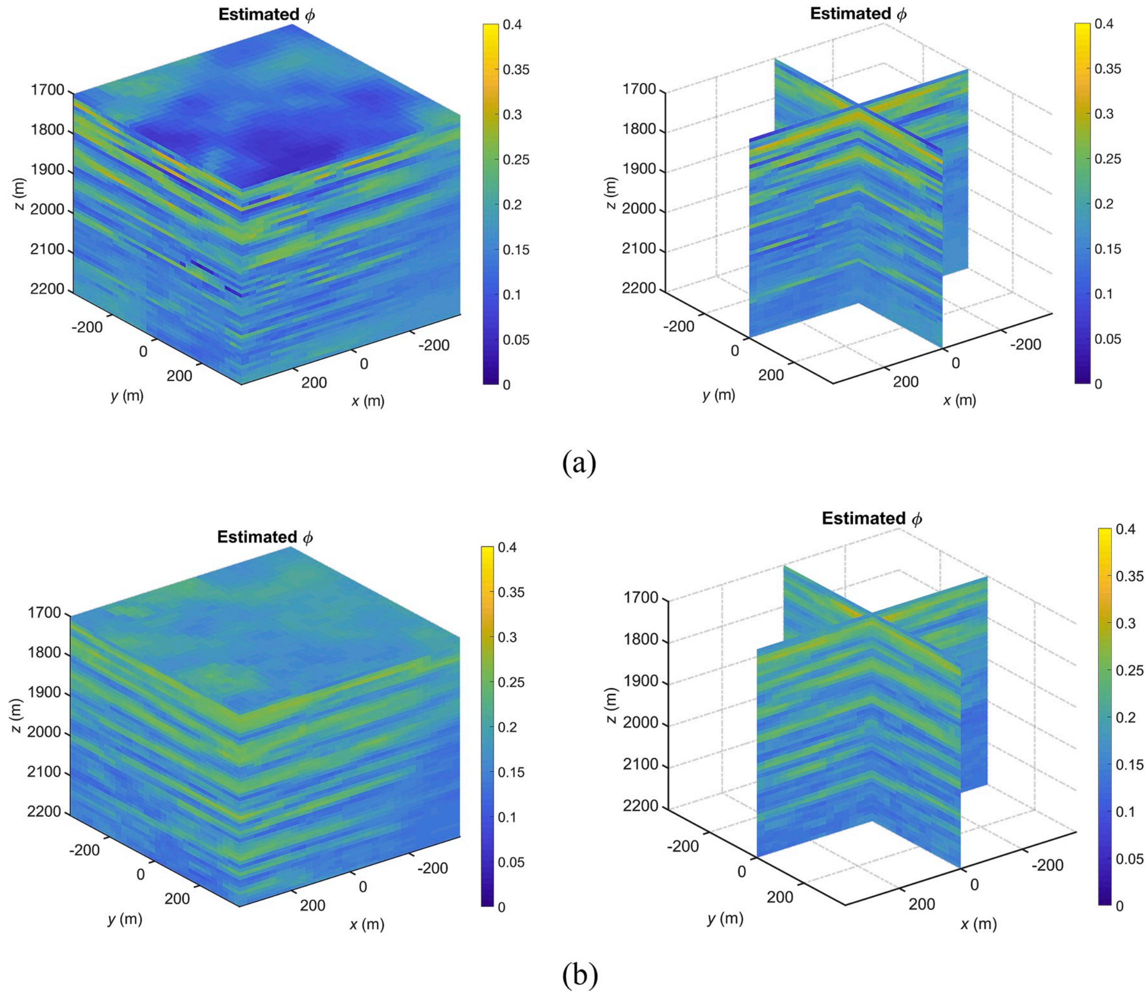

Fig. 11. Estimated porosity by ANN (a) and CNN (b) with the cube inversion results as inputs (Fig. 7b and c).

procedure to explore various distributions of reservoir porosity, and geologically realistic training datasets could be generated through petrophysical models, in which the physical rules imposed by depositional processes should be captured (Das et al., 2019).

After training, predicted porosities by CNN and ANN based on the inversion results of the two wells (Fig. 6) are shown in Fig. 10. It can be seen that the prediction by CNN is better than that of ANN, as well as reflected by an increase of correlation coefficient, which is calculated between predicted and true values. Results at Well_01 are better than those at Well_02, which is attributed to the fact that inversion quality of Well_01 is higher than that at Well_02. It should be pointed out that logging data of Well_01 and Well_02 have to be combined together in order to include the data variability as much as possible, for the training purpose of neural parameters. The aim in this study is to use seismic inversion results as inputs for the prediction of reservoir porosity, which have been kept untouched during the training process. Hence, the predictions with inputs of inverted rock properties at wells could be regarded as a pseudo blind test, in which the performance of trained networks can be further analyzed.

Then, with the cube inversion results as inputs (Fig. 7b and c), porosity estimation can be performed without the limitation of well locations and the whole target of reservoir porosity is obtained (Fig. 11). Both of results share similar patterns, even though differences can be observed, especially for the ones at the top. Note that application of trained systems on the inversion results is instant, and computational time of the networks is mainly attributed to the training process.

6. Discussion

In this paper, in order to exclude the location limitation of wells, results from a full-waveform inversion scheme are proposed as inputs for the estimation of reservoir porosity. Instead of using pre- or post-stack seismic attributes, the non-linear relationship between seismic data and rock properties is explored, since multiples and wave-mode conversions are considered (Fig. 2).

However, due to some problems such as mismatch in the seismic-to-well tie (Fig. 5b), the inversion results are mediocre, even though in the upper part, the match is quite good (Fig. 6). The quality of inverted M is worse than that of κ which is attributed to the fact that only PP data are available here and PS data are rarely collected in real cases (Feng et al., 2017). To further improve the inversion quality, three-component seismic data could be acquired in the field. More importantly, the quality of seismic-to-well match should be increased such that the seismic data can be chosen according to the well trajectory path, or a perturbation mechanism is adopted to stretch or squeeze the logs based on anchoring points (Bakrac et al., 2015).

The internal relationship between reservoir parameters such as porosity ($\varnothing$) and rock properties (κ, M) is being investigated with different neural networks (CNN and ANN), which could help to take the data manipulation to an intelligent level. Compared with other rock physical models (Avseth et al., 2010) where certain assumptions have to be made such as a constant cement of minerals for all depths, these methods do not need any prior knowledge or initial model and are totally data-driven. Another advantage of the proposed deep learning approach is that once the neural weights and biases are fixed after the training process, the trained system can be instantaneously applied to other seismic inversion results, as long as the data distributions, in terms of rock properties and reservoir parameters, are similar.

With 2D filters convolved in the noise-resistant CNN, adjacent information inside the interval window of filters is captured and utilized for the prediction of porosity. As a natural process of deposit and diagenesis, reservoir porosities have intrinsic connections with rock properties in a short depth range. After a consideration of this local knowledge, CNN is performed better than ANN, since the latter one does not use any adjacent information, and it is more sensitive to noises/errors in those inverted rock properties.

Moreover, the inverted κ and M are used together for the porosity prediction in this paper, even though the second one has a lower inversion quality. These two rock properties could be applied respectively, for the training of neural networks. However, large uncertainty may be introduced, since the data relationship will be highly non-linear, or non-unique.

Design of neural architectures and fine-tuning of hyper-parameters are important for a successful retrieval of reservoir porosity, in which a trial-and-error procedure can be applied (Hall, 2016). An early stopping could also be done to reduce the training time and prevent the overfitting problem, when the training error is not becoming smaller during the iterations.

By minimizing a predefined cost function, the training step in deep learning methods only estimate a set of neural parameters through a non-linear regression, which means that only a single value can be predicted for given each input observational data. However, quantitative interpretations require the uncertainty analysis associated with the prediction, in which the posterior distributions need to be sampled for response variables. The technique of approximate Bayesian computation could be utilized, especially in cases where the likelihood distribution is statistically intractable (Das et al., 2019), and will be performed in a future research.

Similar porosity patterns have been produced by these two networks in which the connectivity can be clearly observed in slices (Fig. 11), as demonstrated by high values of porosities ($> 20\%$) in smaller intervals, usually with sand presences. Barriers with $< 5\%$ porosities are acting as traps between potential reservoir units. These observations are conformable with the depositional environments of shallow marine and limnic origins with sand sheets and impermeable shales in-between in the Vienna Basin.

The inversion scheme and neural networks presented here are performed in a trace-by-trace manner, which means that the whole dataset can be divided into sub-volumes in order to speed up on the computation time.

7. Conclusion

To conclude, the location limitation of logged wells has been removed by using inversion results from seismic data for the prediction of reservoir porosity. Thus, 2D sections or 3D cubes of the whole target reservoir can be obtained. The prediction quality of porosity is highly dependent on the input inversions. The non-linear full-waveform inversion scheme applied here could provide a high resolution of rock properties, which are better parameters for the inference of porosity.

Different regression neural networks are used to investigate the complex relationship between rock properties and reservoir parameters, which can be considered as one type of statistical methods, even though they are much more intelligent than others. Convolutional Neural Networks considers the special coupling between reservoir porosity and rock properties with kernel filters, and a higher prediction quality is achieved, compared to that by Artificial Neural Networks.

Declaration of competing interest

The authors declare that they have no known competing financial interests or personal relationships that could have appeared to influence the work reported in this paper.

CRediT authorship contribution statement

Runhai Feng: Methodology, Visualization, Formal analysis, Writing - original draft, Writing - review & editing.

Acknowledgements

This research is sponsored by the DELPHI Consortium. The inversion of seismic data is under the help from Panos Doulgeris of Delft Inversion. The author would like to thank OMV for the permission to publish this data. Comments and suggestions from Prof. A. Gisolf and Prof. A.W. Martinius are also appreciated.

Appendix A. Supplementary data

Supplementary data to this article can be found online at https://doi.org/10.1016/j.jngse.2020.103270.

References

Avseth, P., Mukerji, T., Mavko, G., Dvorkin, J., 2010. Rock-physics diagnostics of depositional texture, diagenetic alterations, and reservoir heterogeneity in high-porosity siliciclastic sediments and rocks — a review of selected models and suggested work flows. Geophysics 75 (5), A31–A47.

Bakrac, S., Gisolf, A., Doulgeris, P., Rizzuti, G., Verschuur, D.J., 2015. Automated full waveform seismic-to-well tying. In: 77th Annual International Meeting of European Association of Geoscientists and Engineers (Expanded Abstract), Madrid, 1-4 June.

Bishop, C.M., 1995. Neural Networks for Pattern Recognition. Oxford University Press, New York.

Biswas, R., Sen, M.K., Das, V., Mukerji, T., 2019. Prestack and poststack inversion using a physics-guided convolutional neutral network. Interpretation 7 (3), SE161–SE174.

Das, V., Pollack, A., Wollner, U., Mukerji, T., 2019. Convolutional neural network for seismic impedance inversion. Geophysics 84 (6), 1–66.

Deng, L., Yu, D., 2014. Deep learning: methods and applications. Found. Trends Signal Process. 7, 3–4.

Feng, R., Luthi, S.M., Gisolf, A., Sharma, S., 2015a. An outcrop-based detailed geological model to test automated interpretation of seismic inversion results. In: 77th Annual International Meeting of European Association of Geoscientists and Engineers (Expanded Abstract), Madrid, 1-4 June.

Feng, R., Luthi, S.M., Gisolf, A., Sharma, S., 2015b. Non-linear full-waveform inversion (FWI-res) of time-lapse seismic data on a higher-resolution geological and petrophysical model, Book Cliffs (Utah, USA). In: 85th Annual International Meeting of Society of Exploration and Geophysics (Expanded Abstract), New Orleans, 18-23 November.

Feng, R., Luthi, S.M., Gisolf, A., 2016a. Lithology prediction from the results of full elastic wave-equation based inversion scheme. In: 78th Annual International Meeting of European Association of Geoscientists and Engineers (Expanded Abstract), Vienna, 30 May-2 June.

Feng, R., Luthi, S.M., Gisolf, A., Sharma, S., 2016b. Lithology prediction based on the full-waveform inversion results. In: International Conference and Exhibition, Barcelona, Spain, 3-6 April.

Feng, R., Luthi, S.M., Gisolf, A., Sharma, S., 2017. Obtaining a high-resolution geological and petrophysical model from the results of reservoir-oriented elastic wave-equation based seismic inversion. Petrol. Geosci. 23, 376–385.

Feng, R., Luthi, S.M., Gisolf, A., Angerer, E., 2018a. Reservoir lithology classification based on seismic inversion results by hidden Markov models: applying prior geological information. Mar. Petrol. Geol. 93, 218–229.

Feng, R., Luthi, S.M., Gisolf, A., Angerer, E., 2018b. Reservoir lithology determination by hidden Markov random fields based on a Gaussian mixture model. IEEE Trans. Geosci. Rem. Sens. 56 (11), 6663–6673.

Fokkema, J.T., van den Berg, P.M., 1993. Seismic Application of Acoustic Reciprocity. Elsevier, Amsterdam, p. 350.

Gibbs, M.N., MacKay, D.J.C., 2000. Variational Gaussian process classifiers. IEEE Trans. Neural Network. 11 (6), 1458–1464.

Gisolf, A., Verschuur, D.J., 2010. The Principles of Quantitative Acoustical Imaging. EAGE Publications b.v., Houten.

Gisolf, A., van den Berg, P.M., 2010a. Target oriented non-linear inversion of seismic data. In: 72nd Annual International Meeting of European Association of Geoscientists and Engineers (Expanded Abstract), Barcelona, 14-17 June.

Gisolf, A., van den Berg, P.M., 2010b. Target-oriented non-linear inversion of time-lapse seismic data. In: 80th Annual International Meeting of Society of Exploration and Geophysics (Expanded Abstract), Denver, 17-22 Oct.

Gisolf, A., Huis in't Veld, R., Haffinger, P., Hanitzsch, C., Doulgeris, P., Veeken, P.C.H., 2014. Non-linear full wavefield inversion applied to carboniferous reservoirs in the Wingate Gas Field (SNS, Offshore UK). In: 76th Annual International Meeting of European Association of Geoscientists and Engineers, Amsterdam, 16-19 June.

Glorot, X., Bengio, Y., 2010. Understanding the difficulty of training deep feedforward neural networks. In: Proceedings of the 13th International Conference on Artificial Intelligence and Statistics, pp. 249–256.

Haffinger, P., 2013. Seismic Broadband Full Waveform Inversion by Shot/receiver Refocusing. Ph.D. Thesis. Delft University of Technology, Delft.

Haffinger, P., von Wussow, P., Doulgeris, P., Henke, C., Gisolf, A., 2015. Reservoir delineation by applying a nonlinear AVO technique - a case study in the Nile Delta. In: 77th Annual International Meeting of European Association of Geoscientists and Engineers (Expanded Abstract), Madrid, 1-4 June.

Hall, B., 2016. Facies classification using machine learning. Lead. Edge 35 (10), 906–909.

Jozanikohan, G., Norouzi, G.H., Sahabi, F., Memarian, H., Moshiri, B., 2015. The application of multilayer perceptron neural network in volume of clay estimation: case study of Shurijeh gas reservoir, Northeastern Iran. J. Nat. Gas Sci. Eng. 22, 119–131.

Kennett, B.L.N., 1983. Seismic Wave Propagation in Stratified Media. Cambridge University Press, Cambridge.

Kingma, D.P., Ba, J., 2014. Adam: A Method for Stochastic Optimization arXiv preprint arXiv:1412.6980.

Kováč, M., Sliva, L., Sopková, B., Hlavatá, J., Škulová, A., 2008. Serravallian sequence stratigraphy of the northern Vienna Basin: high frequency cycles in the Sarmatian sedimentary record. Geol. Carpathica 59, 545–561.

Lima, R.P., Suriamin, F., Marfurt, K.J., Pranter, M.J., 2019. Convolutional neural networks as aid in core lithofacies classification. Interpretation 7 (3), SF27–SF40.

Na'imi, S.R., Shadizadeh, S.R., Riahi, M.A., Mirzakhanian, M., 2014. Estimation of reservoir porosity and water saturation based on seismic attributes using support vector regression approach. J. Appl. Geophys. 107, 93–101.

Nair, V., Hinton, G.E., 2010. Rectified linear units improve restricted Boltzmann machines. In: Proceedings of the 27th International Conference on Machine Learning, pp. 807–814.

Rolon, L., Mohaghegh, S.D., Ameri, S., Gaskari, R., McDaniel, B., 2009. Using artificial neural networks to generate sysnthetic well logs. J. Nat. Gas Sci. Eng. 1 (4–5), 118–133.

Strauss, P., Harzhauser, M., Hinsch, R., Wagreich, M., 2006. Sequence stratigraphy in a classic pull-apart basin (Neogene, Vienna Basin). A 3D seismic based integrated approach. Geol. Carpathica 57, 185–197.

Tarantola, A., 1984. Inversion of seismic reflection data in the acoustic approximation. Geophysics 49, 1259–1266.

Tetyukhina, D., Luthi, S.M., Gisolf, D., 2014. Acoustic non-linear full-waveform inversion on an outcrop-based detailed geological and petrophysical model (Book Cliffs, Utah). Am. Assoc. Petrol. Geol. Bull. 98, 119–134.

Treister, E., Haber, E., 2017. Full waveform inversion guided by travel time tomography. SIAM J. Sci. Comput. 39, S587–S609.

Virieux, J., Operto, S., 2009. An overview of full-waveform inversion in exploration geophysics. Geophysics 74, WCC1–WCC26.

White, R.E., 2003. Tutorial: good practice in well ties. First Break 21, 75–83.

Wu, J., Yin, X., Xiao, H., 2018. Seeing permeability from images: fast prediction with convolutional neural networks. Sci. Bull. 63, 1215–1222.

Wu, Y., McMechan, G.A., 2018. Feature-capturing full waveform inversion using a convolutional neural network. In: 88th Annual International Meeting of Society of Exploration and Geophysics (Expanded Abstract), Anaheim, 14-19 Oct.

Yang, D., Liu, F., Morton, S., Malcolm, A., Fehler, M., 2016. Time-lapse full-waveform inversion with ocean-bottom-cable data: application on Valhall field. Geophysics 81, R225–R235.

Yang, F., Ma, J., 2019. Deep-learning inversion: a next-generation seismic velocity model building method. Geophysics 84 (4), R583–R599.

Yu, H., Wang, Z., Rezaee, R., Zhang, Y., Han, T., Arif, M., Johnson, L., 2018. Porosity estimation in kerogen-bearing shale gas reservoirs. J. Nat. Gas Sci. Eng. 52, 575–581.